Experimental and instrumentation

2.1 Introduction

This chapter deals with the brief outline about the materials synthesis, sample preparations via LB/LS method and their characterization techniques. PIn and its derivative poly(5-aminoindole) (5-APIn) were polymerized from their respective monomers via chemical, electrochemical and interfacial routes. Poor solubility of this PIn family in common volatile organic solvents have plagued them for practical applications and fabrication of devices. Though, various nanocomposites of PIn have been prepared which exhibit good electro catalytic activity, photoelectrochemical property as well as better electrical properties [69,78-83]. Still, the issue of solution processability and poor conductivity hang on the major limiting factor for its broad practical applications. In this thesis, we tried to resolve the processability issue of unsubstituted PIn and substituted PIn to much extent by employing the concept of co-solvent methodology i. e. dissolving in one solvent (dimethyl sulfoxide; DMSO) which acts as good solvent followed by transfer in other common volatile organic solvent (chloroform). LB technique necessitates the material solubility in volatile solvent that is immiscible with water for uniform spreading over water subphase. DMSO being a very good polar solvent capable of solubilizing nitrogen containing polymers without much affecting the material is associated with the demerit of higher boiling point and some miscibility with water. We then took the wealth of DMSO for being miscible with chloroform and accomplished the prerequisite of LB sample preparation. After that, we explored LB technique to obtain its stable and well-ordered film (without utilizing any external template) with very smooth surface and further investigated its layer dependent charge transport property and better electronic device parameter.

The polymer synthesized was characterized for its formation and stability via ^{1}H-NMR, FT-IR, UV-Vis. Spectroscopy, TGA/DTA. LB and LS technique were employed to deposit the film of PIn and 5-APIn polymers over various substrates. These LB/LS films were characterized via UV-vis. and raman spectroscopy for ordering (π-π stacking) enhancement. Their large area film uniformities were investigated via Scanning Electron Microscopy (SEM), TEM, Atomic force microscopy (AFM) and phase imaging, and finally electrical parameters were studied.

2.2 Experimental

2.2.1 Materials

Indole (In) monomer, 5-Aminoindole (5-AIn), ammonium persulfate ($(NH_4)_2S_2O_8$, APS), TBAP (tetrabutylammonium perchlorate), sodium molybdate ($Na_2MoO_4.2H_2O$), L-Cysteine ($HO_2CCH(NH_2)CH_2SH$), Silver Nitrate ($AgNO_3$, anhydrous), Sodium Borohydride ($NaBH_4$, anhydrous), Didodecyldimethylammonium bromide (DDAB) were purchased from Sigma Aldrich, India. Milli-Q (resistivity = 18.0 Ω cm^{-1} and pH=7.0) water has been used in all experiments. Acetonitrile, DMSO, chloroform and distilled water were obtained from Merck, India. All chemical were used as procured without any further purification/processing.

2.2.2 Chemical (single phase) synthesis of PIn

There are many protocols reported for the chemical synthesis of PIn utilizing various oxidants [69]. In this thesis, the *in-situ* oxidative chemical polymerization has been carried out by dissolving 0.05 M indole monomer in minimal volume of ethanol and adding it to pre ice-cooled (~5ºC), nitrogen purged 0.1N HCl in a stoppered conical flask [71,72]. Then 0.1 M APS solution (in 5mL distilled water) was added dropwise to the

above system with continuous stirring. This setup was kept on stirring over night (24 h) in ice-bath (~5ºC) for complete polymerization. The green precipitate so obtained was allowed to settle down before it was filtered and washed with water and ethanol several times. The final product was dried under vacuum and yield was calculated. Similar protocol is followed for substituted PIn such as 5-APIn [69] Figure 2.1 demonstrates the reation scheme and the reaction mechanism is already discussed in section 1.6.2.1.

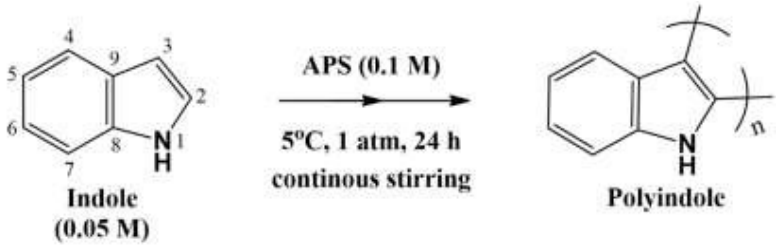

Figure 2.1 Reaction scheme for the synthesis of PIn.

2.2.3 Electrochemical synthesis of PIn

Electropolymerization was carried out in a three electrode cell assembly consisting of Au as working, platinum (Pt) as counter and Ag/AgCl (at 1.2 V) as reference electrodes (as shown in Figure 2.2) were used for the electrochemical polymerization. 0.1 M TBAP in acetonitrile was employed as supporting electrolyte which was N_2 purged prior to synthesis [55,69]. After the polymerization, the coated Au electrode was quickly rinsed in acetonitrile to wash out unreacted monomer and electrolyte. The dried polymer was carefully removed from the electrode and was used further for LB film preparation. Similarily, reports on electrochemical synthesis of 5-APIn is also available [86,87]. 5-APIn synthesized electrochemically undergoes irreversible degradation on application of oxidizing potentials greater than 0.6 V. This phenomena of loss in electrochromic properties at potentials greater than 0.6 V is due to over-oxidation [86-89]. Therefore, another synthesis technique i.e. interfacial technique was employed that yielded

morphology controlled polymer in bulk with excellent electroactivity even at higher positive potentials described in detail chapter 4.

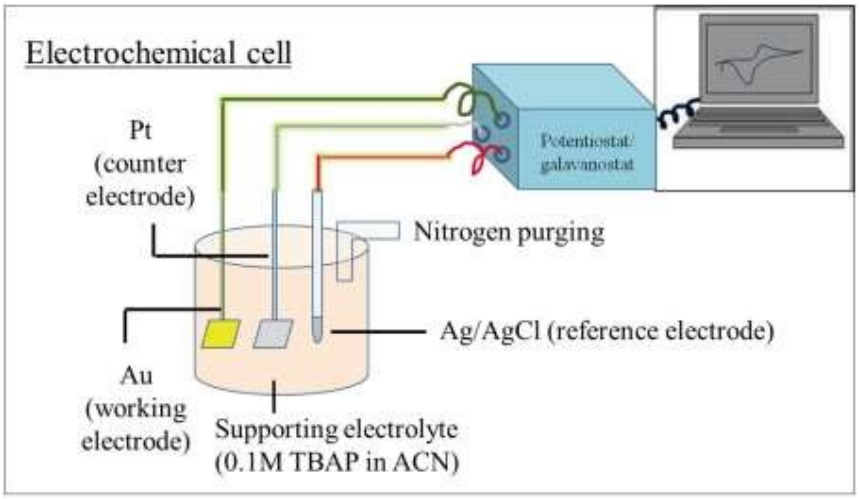

Figure 2.2 Experimental setup for electrochemical synthesis of PIn.

2.2.4 Interfacial (biphase) synthesis of 5-APIn

The interfacial synthesis method for 5-APIn synthesis was carried out using following protocol in a 30 mL vial at room temperature (25 ± 1 °C). Two immiscible solvents chosen here were chloroform and water. Initially, 0.06 M 5-AIn monomer was dissolved in 4.0 mL chloroform. To this, a freshly prepared solution of APS (0.1 M, 8.0 mL) in double distilled water was added drop-wise along the wall of the vial under non-stirring condition. Gradually, a dark brown ring (initiation of polymerization) was observed at the interface (red circle in (b) Figure 2.3) which increased in width simultaneously with the addition of APS. The interfacial system formed had upper aqueous layer containing oxidizing agent (APS) and bottom organic layer containing monomer. After the complete addition of APS, the vial was sealed, covered with aluminum foil and left undisturbed for 24 h. The upper aqueous layer was then carefully removed using pipette without disturbing the interface. The solid polymer (protonated

form) was then collected by centrifugation followed by multiple washings with de-ionised water (to deprotonate amino group and remove excess of oxidizing agent) and then with chloroform (to remove unreacted monomer). Finally, the polymer was dried under vacuum and yield of the product was reported as 85%. Similar procedure is followed for interfacial synthesis of unsubsituted PIn [72].

Figure 2.3 Schematic representation of interfacial polymerization of 5-AIn at aqueous/organic solvent system. The top phase is an aqueous solution of APS and bottom phase is monomer/Chloroform solution.

2.2.5 Composite formation of PIn

2.2.5.1 Hydrothermal synthesis of MoS_2 nanosheets and formation of MoS_2-PIn composite

MoS_2 nanosheets are synthesized using facile, single step hydrothermal method as displayed in Figure 2.4 [90]. Sodium molybdate ($Na_2MoO_4.2H_2O$) and L-cysteine ($HO_2CCH(NH_2)CH_2SH$) (1:2 w/w) are dissolved in 25 ml of Milli-Q water in separate beakers and kept on constant stirring for 15 minutes. Then the two solutions are mixed

slowly with continuous stirring maintaining temperature at ~40°C and pH at 3.0 with concentrated HCl. This solution is then transferred into stainless steel lined Teflon autoclave (100 ml capacity) maintained at ~200°C for 42 hours. After this, the content is left to cool down naturally, finally we obtain dark brown precipitate (nanosheets) settled at the bottom. These nanosheets were washed repeatedly via centrifugation and re-dispersion in water to obtain the final product. For the *in-situ* oxidative chemical polymerization of indole monomer, MoS_2 nanosheets (0.4 mg/mL) were added to the indole solution (ethanol-water mixture) prior to addition of APS. Then this system was subjected to ultrasonication for 30 min followed by dropwise addition of APS solution (0.1 M in 5mL distilled water) with continuous stirring. Rest steps were the same followed during chemical polymerization of In (discussed in section 2.2.2). The final product was dried under vacuum and yield was calculated as 74%.

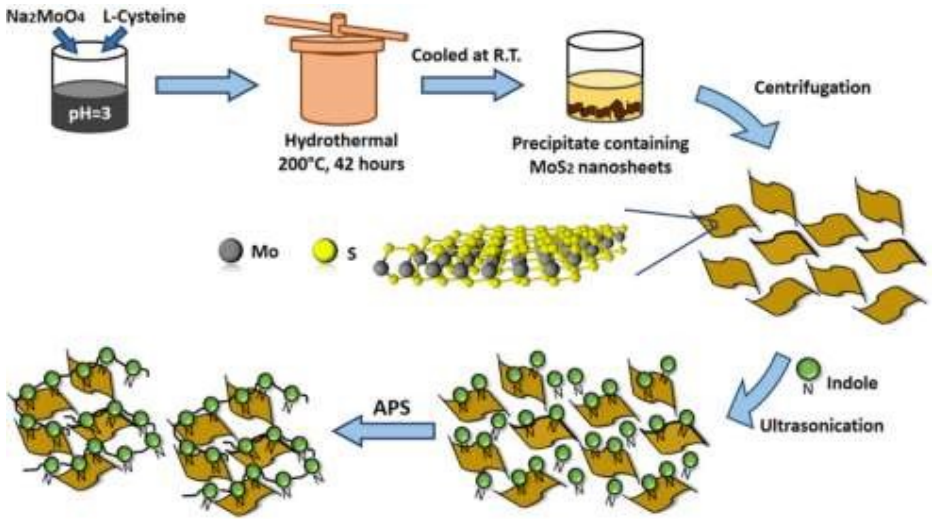

Figure 2.4 Schematic representation of hydrothermal synthesis of MoS_2 nanosheets, their exfoliation, and MoS_2-PIn nanocomposite formation.

We have proposed a plausible mechanism for green synthesis of MoS_2 nanosheets utilizing sodium molybdate and L-cysteine as precursors. Overall the reaction in

hydrothermal reactor can be said to involve four main steps: (1) Hydrolysis of L-cysteine, (2) conversion of MoO_4^{2-} to MoO_xS_{4-x}, (3) acid catalysed formation of MoS_3, (4) formation of MoS_2 nanosheets. This complex process can be expressed as follows:

$$HO_2CCH(NH_2)CH_2SH + H_2O \rightarrow CH_3COCOOH + NH_3 + H_2S \quad (1)$$

$$MoO_4^{2-} + HS^- \rightarrow MoO_xS_{4-x} + H_2O \quad (2)$$

$$MoO_xS_{4-x} + H^+ \rightarrow MoS_3 \quad (3)$$

$$MoS_3 \xrightarrow{\Delta} MoS_2 \quad (4)$$

We have employed controlled experimental conditions (such as pressure and temperature) provided by hydrothermal set up along with presence of reducing agent (twice the molar ratio that of molybdate) in the vicinity that provides enough S^{2-} for replacing lattice O^{2-} at the immediate site. There is also possibility of formation of octa molybdates. These controlled conditions prevent its formation thus favoring the formation of MoS_2. The role of low pH here is to catalyse/accelerate the reaction step (3) mentioned above.

2.2.5.2 Synthesis of AgNPs, their liquid-liquid phase transition and composite formation with PIn

The synthesis was done through reduction of silver salt with sodium borohydride where all the components were taken in solution form prepared in deionised water. A 10 mL of 0.001 M $AgNO_3$ solution prepared in deionized water was added at rate of one drop per second to a 30 mL 0.002 M solution of freshly prepared $NaBH_4$ in a 200 mL borosilicate beaker under constant stirring (1100 rpm). The $NaBH_4$ solution beaker is kept in an ice bath at all times to prevent it from degrading or reacting with water. After a few drops of $AgNO_3$ solution being added to the system the colour is seen to change to a light yellow and keeps getting darker with further addition of $AgNO_3$ solution. Stirring is stopped as soon as all the $AgNO_3$ has been added to the borohydride solution and a dark yellow clear

solution is obtained. This solution is analysed through UV-Vis and TEM for its formation. AgNPs from the prepared Ag hydrosol are then transferred to an organic phase using DDAB as phase transfer agent (PTA). Various concentrations of DDAB solution, namely 5, 10, 25, 50 and 75 mM are prepared in chloroform. 5mL of these solutions are kept in a 30 mL capped borosilicate vial. A same volume of Ag hydrosol is added slowly to all the above vials along the walls. Initially, a distinct biphasic system is obtained as shown in Figure 2.5 (a) with clear chloroform phase at the bottom and dark yellow hydrosol above it due to immiscibility and density differences of water and chloroform. Immediately the vial is then capped well to prevent any leakage and shaked vigorously (for 120 secs) to facilitate maximum interface formation for phase transfer. Vigorous shaking provides sufficient kinetic energy to DDAB capped AgNPs cross the interface barrier. The mixture in the vial is allowed to rest and stabilize to obtain the biphasic system with chloroform phase gaining yellow colour while dark yellow from the aqueous phase turns lighter (Figure 2.5 (b)). As it is evident from Figure 2.5 (b), we observe difference in colour intensity after phase transfer for varying DDAB concentration. In absence of DDAB addition into chloroform (control experiment) no phase transfer occured that clearly demonstrates the interactions between silver nanoparticles and DDAB facilitates phase transfer. The difference in colour intensity of the bottom phase clearly supports our speculation that DDA+ induced phase transfer is size dependent. This observance is in agreement with the TEM characterizations mentioned in detail in Chapter 6. DDAB surfactant aided phase transfer of NPs as well as its stabilization in the organic phase studied for various DDAB concentrations, out of which 25 mM concentration appeared to exhibit maximum number and almost uniform size of particles transferred into the organic phase (Figure 6.6).

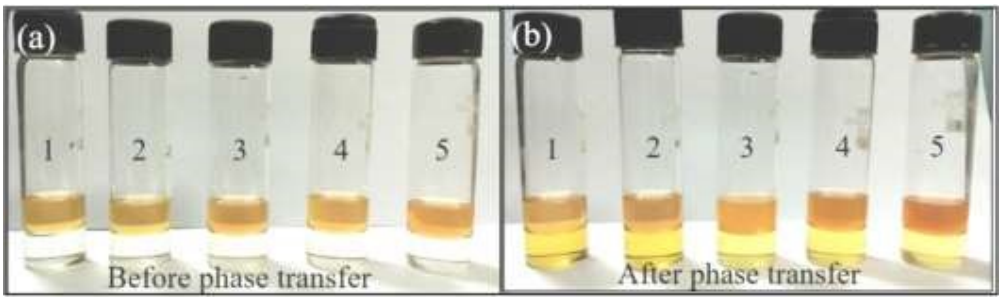

Figure 2.5 Biphasic system with chloroform at bottom containing various DDAB concentration labelled as (1) 5, (2) 10, (3) 25, (4) 50 and (5) 75 mM and upper layer containing hydrosol (a) Before phase transfer (b) After phase transfer.

PIn was chemically synthesized following the same procedure as detailed in section 2.2.2. The as synthesized PIn was dispersed in DMSO (polar and slow evaporating solvent) followed by addition of Ag organosol having concentration up to ~1 mg/mL which was utilized further for spreading on water subphase for LS film deposition.

2.3 Sample preparation techniques by LB/LS method

Polymer and their composites synthesised via chemical, electrochemical and interfacial route were then used for formation of LB/LS film over various substrates. As synthesized PIn, 5-APIn and their composites did not give a true dispersion in chloroform, therefore 10 mg/mL solution was prepared first in DMSO followed by addition of chloroform (in ratio 1:10) to obtain a true dispersion of 1.0 mg/mL concentration. LB trough and the barrier were cleaned with detergents and wiped off. The next step was solvent cleaning process with acetone, ethanol and chloroform in sequence followed by rinsing with distilled water. Then the trough was filled with water distilled water and left undisturbed for few hours. This waiting was necessary because while cleaning the trough there might be some stray left on the trough wall which may take time to leech up to the air-water interface [53,54].

It is very necessary to remove the stray contaminants before spreading of the sample on the water subphase. Air-water interface cleaning is done via suction pump to ensure that SP attains zero value prior to sample spreading. Next step is the substrate cleaning process such as unmodified ITO (hydrophilic nature), via ultrasonication in acetone, chloroform and water, for 15 min respectively and drying in vacuum. Prior to formation of ordered LB film of polymer, π-A isotherm must be investigated to interpret the interaction between polymer chains (intermolecular and intramolecular interactions) and film stability at the air-water interface. Then the sample is spread on the water subphase (pH=7.0, ρ=18.0 Ω cm^{-1}, T~ 25 °C) of trough with working area 650 mm x 200 mm (Model No. LB-2007DC; Apex) fitted with double barrier. Spreading was done with Hamilton syringe (drop rate=50 μL/min). The LB system with WinLB software provides expansion/compression resolution of 0.005 mm and surface pressure resolution of ±0.02 mN/m. The films are deposited on solid substrates at an optimum SP obtained from their respective isotherms.Films are lifted either vertically (Blodgett style) at a speed of 3 mm/min or stamped (LS) and dried in an inert (N_2) atmosphere (glove box).

2.4 Characterizations

Instrumentation and characterization techniques utilized in this thesis are as follows.

Figure 2.6 Photograph of LB film deposition system.

2.4.1 Nuclear magnetic resonance (NMR) spectroscopy

Nuclear Magnetic Resonance (NMR) spectroscopy is used to determine the molecular structure of a sample as well as for determining the purity and content of the sample. Figure 2.7 displays photograph of our NMR instrument Bruker FT-NMR (500 MHz) and basic principle involved in obtaining a spectra. NMR in this thesis has been utilized to

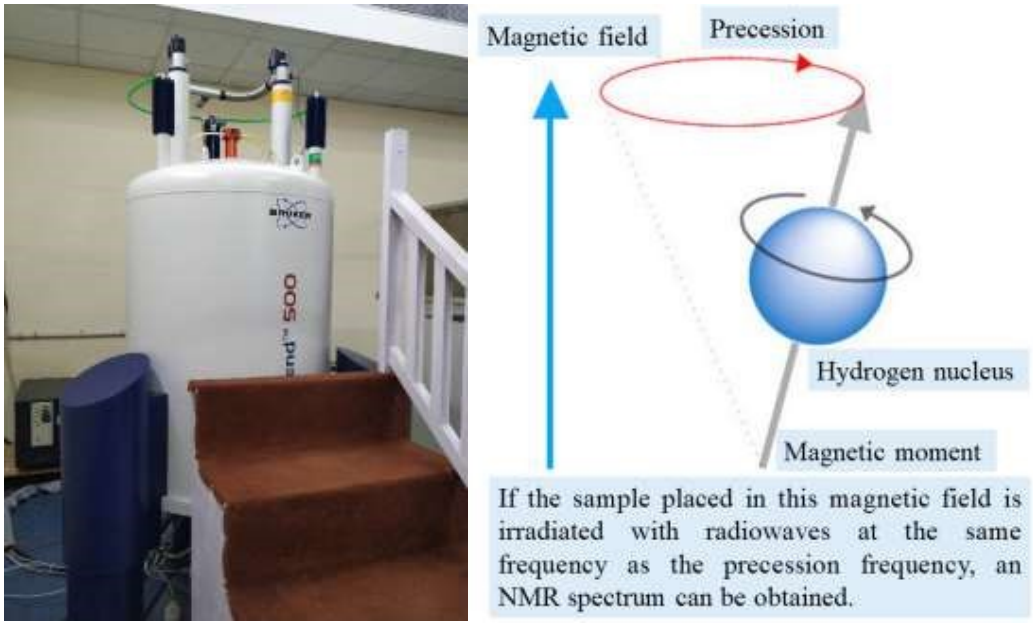

Figure 2.7 Photograph of Nuclear Magnetic Resonance (NMR) spectrometer and its basic working principle.

investigate the polymerization linkages of the monomer units. NMR helps to determine physical properties of the sample at the molecular level such as solubility, phase changes, conformational exchange and diffusion [91,92]. ^{1}H-NMR spectra were recorded in deuterated solvent like DMSO-d^{6} solvent, and chemical shift (δ) was reported in parts per million (ppm).

2.4.2 UV-Vis absorption spectrophotometry

UV-Vis spectroscopy is an important tool to locate the absorption band in materials

science. This absorption or reflectance spectroscopy in the UV-Vis region (normally 200 nm to 1000 nm) directly affects the perceived color of the chemicals involved. The basic principle involved in this electronic spectroscopy is the excitation of electrons from the ground state (G.S.) to the higher energy excited state (E.S.) within the molecule having particular electronic environment shown in Figure 2.8 [91,92].

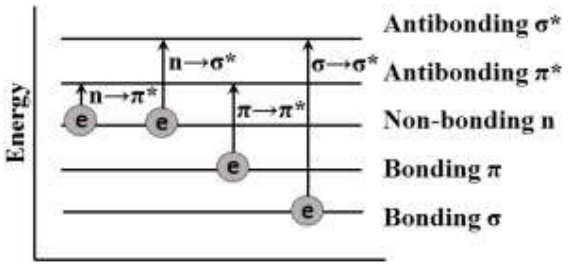

Figure 2.8 Electronic transitions in a molecule.

Among the various possible transitions in a molecule shown in Figure 2.8, most favorable electronic transition occurs from the HOMO to LUMO. Basic instrumentation for UV-Vis spectroscopy is represented as Figure 2.9. According to the Beer-Lambert law, when a monochromatic light with intensity I_0 passes through a solution (absorbing medium) contained in path length of 1 cm, the rate of decrease in intensity is directly proportional to I_0 and the sample concentration. Molecules that contain π-electrons or non-bonding (n) electrons such as heteroatom containing conjugated polymers absorb energy in UV or Vis region and promote these electrons to anti-bonding (higher energy) molecular orbital (Figure 2.8). The more easily these electrons are excited, lower is the energy gap between HOMO and LUMO, and thus longer is the radiation wavelength that it absorbs. This spectroscopy technique is unique in itself for characterizing signature absorptions of noble metals (like Ag, Au) known as surface plasmon resonance (SPR) band which is not present in their bulk metal counterpart or its respective ions. SPR originates from coherent interaction of the electrons in the conduction band of the metal with electromagnetic

radiation. Optical properties of NPs is sensitive to the size, shape, concentration and dielectric environment of the NPs which is easily analysed via this technique [90,91]. As a part of research work we have exclusively utilized UV-Vis technique to locate the absorption spectrum of metal nanostructures and LB/LS films of polymer to investigate extent of conjugation in this thesis. UV-Vis absorption study in this thesis was carried out using Lambda 25 spectrophotometer of Perkin Elmer, Germany.

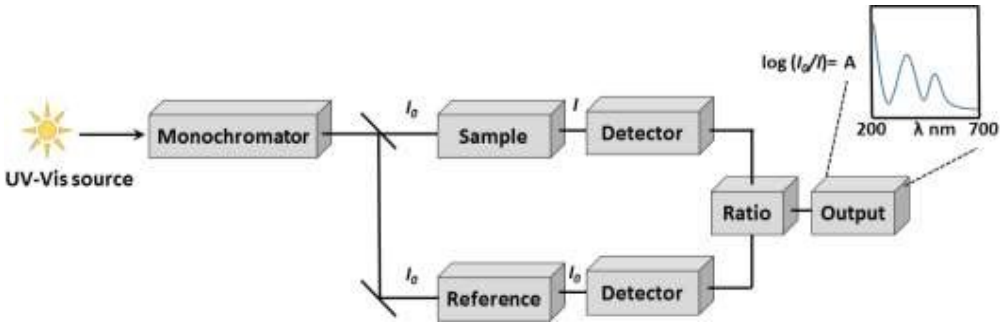

Figure 2.9 Basic instrumentation of UV-Vis spectrometer.

2.4.3 Fourier Transform Infrared spectroscopy

Fourier Transform Infrared spectroscopy (FT-IR) is an important tool which is used to analyze the chemical composition of many organic compounds, biological samples, polymers and inorganic minerals. Wide range of sample materials in bulk or thin films,

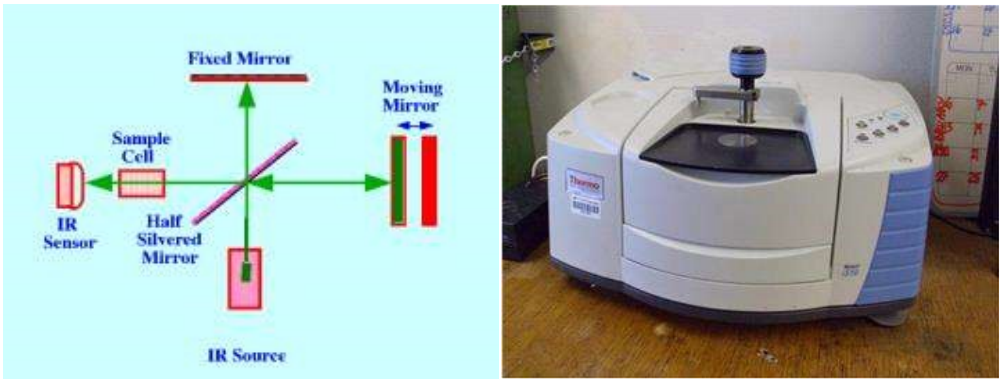

Figure 2.10 (a) A simple schematic diagram of the FT-IR spectrometer (b) Photograph of FT-IR spectrometer.

liquid, solid (powders), fibers and other forms can be analysed via FT-IR. Like electronic transitions in UV-Vis spectroscopy, vibrational transitions in a molecule also relate to discrete energy levels, thus molecules absorb IR radiation only at definite wavelengths and frequencies [91,92]. Figure 2.10 shows the working principle of FT-IR spectrometer and its photograph. FT-IR spectra for all samples were recorded with a Thermo 5700 FT-IR spectrometer, Germany.

2.4.4 Raman spectroscopy

Raman spectroscopy is a highly versatile, non-destructive chemical analysis technique that is used to observe vibrational and rotational trasitions as well as some low frequency modes of a system. This technique is also known to provide structural fingerprint of a molecule. It is based on inelastic scattering (Raman scattering) of monochromatic radiation interacting with the sample. [91,92]. In this work, Micro Raman Spectrometer (Renishaw, Germany) at 1800 scattering geometry attached with an Ar^+ laser (514.5 nm, 50 mW) was used to investigate the polymer PIn LB/LS films for polymer chains ordering, orientation and to compare it with the electrochemically formed starting material, PIn. Photophysical properties of polymer-metal nanoparticle coupled unified system via Surface-enhanced Raman Spectroscopy (SERS) has been observed and discussed. Raman spectra of LB/LS films have been investigated on WITec (alpha 300, India.

2.4.5 X-ray photoelectron spectroscopy

X-ray photo electron spectroscopy (XPS) or electron spectroscopy for chemical analysis (ESCA) is basically the irradiation of a sample surface with monochromatic X-rays. Figure 2.11 illustrates the schematic presentation of the physical process involved in XPS based on the photoelectric effect.

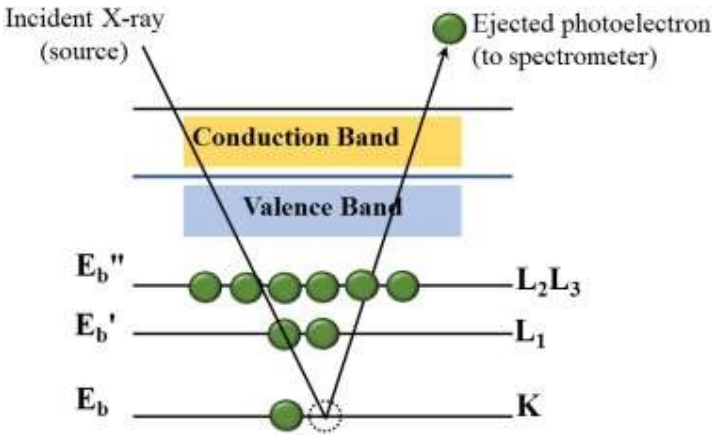

Figure 2.11 Physical process involved in XPS.

Common way of spectroscopic surface measurement comprise the irradiation of sample with a primary beam made up of photon, electrons and impact of this on the surface result in the formation of secondary beam from the substrate which is measured/detected by the spectrometer as shown in Figure 2.11. XPS spectrum thus obtained is the plot of intensity (count/sec) vs. binding energy (eV). Wide scan XPS spectrum is called survey spectrum which generally displays scan from 0 to 1200 eV binding energy. In the present thesis we have utilized XPS spectrum for elemental analysis, identification of oxidation state of the synthesized nanomaterials and their on interaction with polymer on Shimadzu Amicus XPS (UK), Kratos analytical instrument ($\lambda_{Mg\text{-}K\alpha}$=1.254 Å radiation).

2.4.6 Cyclic voltammetry

Cyclic voltammetry (CV) is the most extensively used technique for obtaining qualitative details about electrochemical reactions in a system. It offers a rapid location of redox potentials of the electro active species in the system. The experimental setup consists of assembly of three electrodes in cell viz. working, counter and reference electrodes, respectively connected to a power supply (Figure 2.12).

In CV measurement, materials coated over conducting surface are named as working

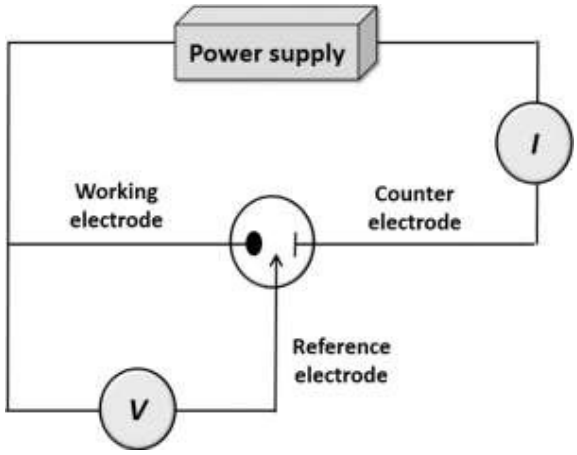

Figure 2.12 Schematic representation of the experimental setup of CV.

electrode while noble metal like platinum/gold is used as counter electrode to complete the circuit. Ag/AgCl is used as reference electrode in order to measure the working electrode potential. The voltage is scanned between two sets of potential as lower limit and upper limit. After reaching a set potential during CV scan of a system, the potential ramp of working electrode gets inverted to give a cyclic voltammogram. The scanning with constant scan rate between two sets of potential causes appearance of peak/s which gives the level of electron where electron can eject or insert (oxidation or reduction). The peaks of CV can be used to locate the HOMO or LUMO. Formula used to calculate the HOMO is given below

$$E_{HOMO} = [(E_{ox} - E_{1/2(ferrocene)}) + 4.8]\ eV \qquad (2.1)$$

Where Eo_x is obtained from the peak value of current-voltage of CV and $E_{1/2\ (ferrocene)}$ is half oxidation potential of ferrocene [93]. Cyclic voltammograms were recorded with Autolab (PG STAT, 302, The Netherlands, GPES software) using a conventional three-electrode system. Au and Pt electrodes were used as working and counter electrodes respectively. Electrochemical impedance spectroscopy (EIS) was performed at Electrochemical Workstation (CHI7041C, USA). Prior to electrode modification, disc

electrodes (diameter = 2.0 mm) were polished with alumina slurry (particle size = 0.4 μm) over polishing pad. Then it was rinsed with acetone in ultrasonic bath for surface cleaning. Then after, dispersion of the sample (polymer or its composite) was cast over the electrode and left for drying at room temperature.

2.4.7 Thermo Gravimetric Analysis

Thermal Analysis techniques such as thermogravimetric analysis (TGA) and differential thermal analysis (DTA) help to determine rate of change in weight/mass and enthalpy (heat flow) as a function of temperature. This measurement is used primarily used to study the properties of materials with change in temperature and thus help to predict their thermal stability [92]. Thermal stability of samples were investigated by TGA/DTA that is a noteworthy way of studying their thermal degradation behavior. Thermal analysis was carried out on Mettler Toledo (TGA/DSC 1 STARE System, Switzerland) at a heating rate of 20 °C min^{-1} in the inert atmosphere.

2.4.8 Scanning electron microscopy (SEM)

A scanning electron microscope (SEM) (shown in Figure 2.13) gives detail information of the surface topography and elemental composition of the sample. The electron beam possessing significant amount of kinetic energy interacts with the sample that produces various signals depending on the penetration depth of the electron beam [91]. Time-dependent growth and morphology of synthesized polymers were studied using SEM instrument of Carl Zeiss, Supra 40, Germany (operating voltage 2-15 kV). The structural information of the polymer LB/LS films were obtained using High resolution SEM (Nova Nanosem 450 FEI, Netherlands).

2.4.9 Transmission electron microscopy (TEM)

Photograph shown in Figure 2.14 is a high resolution transmission electron microscope

Figure 2.13 Photograph of our SEM and HR-SEM.

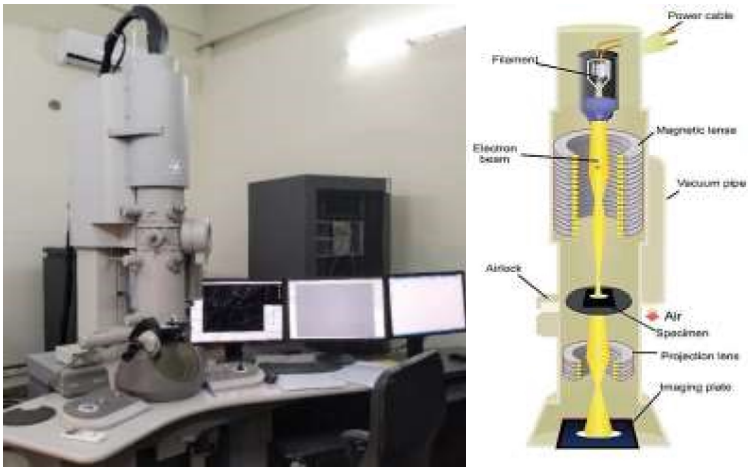

Figure 2.14 (a) Photograph of TEM (b) Layout of optical component of TEM instrument.

(HR-TEM) instrument of model FEI, TECHNAI G^2 20 TWIN (Czech Republic) operating at an accelerating voltage of 200 kV. It is equipped with TEAM EDS SYSTEM with Octane Plus SDD detector for energy dispersive spectroscopy (EDS). Image acquirement and processing were performed using the Gatan Digital Micrograph software. TEM offers nanomaterials imaging giving detailed information about their crystalline structure in selected area electron diffraction (SAED) pattern and elemental composition. As shown in schematic representation in Figure 2.14, TEM works like a light microscope with glass lenses replaced by magnetic coils and the illuminating source

being the electron beam [94]. In this thesis, this technique has been extensively used for investigating MoS_2 nanosheet and AgNPs formation and large area uniform distribution in polymer matrices. Apart from this, LB/LS pristine polymer films lifted at optimum surface pressure on TEM grid informs us about the enhanced crystallinity (π-π stacking distance).

2.4.10 Atomic Force Microscopy

Atomic force microscopy (AFM) provides surface structure (3D) and phase contrast image analysis micrograph of polymer films or various materials such as metals, ceramics, semiconductors, and biological samples. It is a versatile technique that donot requires vacuum condition and presents the interaction of probe (AFM tip) with the sample surface. Surface study of all samples in this thesis were done on scanning probe microscope (SPM) (model: NTEGRA Prima, NT-MDT Services & Logistics Ltd.). Figure 2.15 displays a simple schematic diagram of a typical AFM.

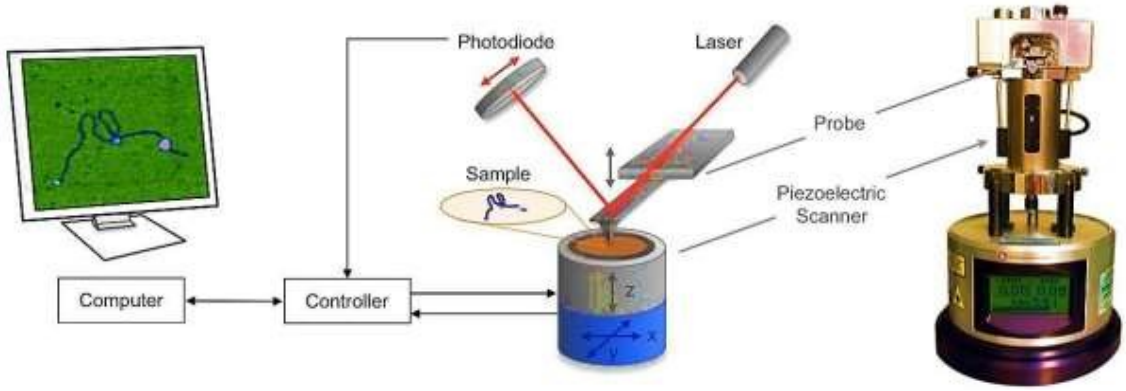

Figure 2.15 A simple schematic diagram of the AFM.

2.4.11 X-ray diffraction

X-ray diffraction (XRD) pattern is a primary technique used in the present work to determine the degree of crystallinity in samples such as nanomaterials, polymer and its composites on a XRD Miniflex 600 diffractometer equipped with CuKα ($\lambda_{K\alpha}$ =1.54056

Å) radiation at a scan rate of 3°/min. It helps in determining the crystallite size in the polymers.

2.5 Device fabrication

The device is fabricated in Sandwich structure ITO/Polymer LB (or LS)/Al (Schottky diode) and process consists of following steps:

2.5.1 Substrate cleaning

ITO is used as substrate for device fabrication. The substrate were cleaned using DI water, acetone, chloroform for 15 min each using ultrasonic bath. The cleaned substrates were for 20 min in vacuum oven at 50 °C.

2.5.2 Thin film deposition

Two techniques have been used for depositions of polymer films over substrate: LB and LS technique. The details about these techniques have discussed in section 2.2.1 & 2.2.2.

2.5.3 Electrode deposition

Vacuum thermal evaporations techniques have been used in present study to deposit metal electrode thin films. In this process, materials are vaporized at low pressure approx. 10^{-6} torr by heating the filament according to material to be evaporated (Figure 2.16). An electric variac is used to monitor the temperature of the filament by controlling the current. There are several parameter which can be varied during the deposition of film such as depositions rate, film thickness, substrate temperature and deposition angle etc.

The diffusion pump backed by rotary pump was used to create vacuum inside the chamber. The thickness of film is controlled by using the quartz crystal micro balance. These processes offer a very clean method of depositions of metal film as electrodes. Circular shadow masking of Al dots (electrode) of diameter 1 mm and thickness of 60 nm monitored via digital thickness monitor (DTM) was achieved on polymer and

nanocomposite LB/LS films via thermal deposition technique (Hind High Vac, India, model: 12A4D) maintaining pressure at $3x10^{-6}$ mbar.

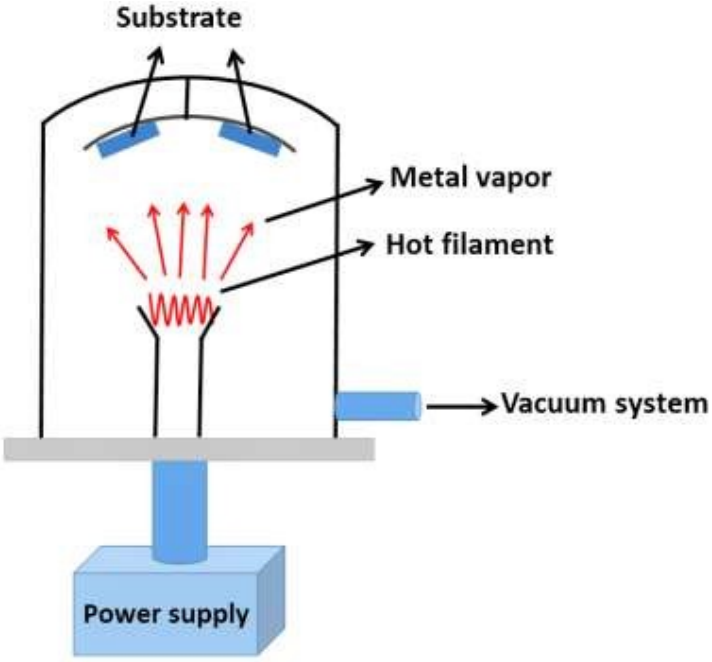

Figure 2.16 Schematic diagram of Thermal Evaporating vacuum system.

2.5.4 Device characterization

Figure 2.17 shows the schematic diagram of ITO/semiconductor LB (or LS) film/Al sandwiched structure for device formation. The measurement of the devices prepared is performed in two probe measurement using source meter Keithley (model 2612A). This sourcemeter unit, interfaced with computer, was used to measure the current (I)- voltage (V) relationship, by varying small step of voltage range while recording the current density through device. A voltage (V) is applied between the electrodes using voltmeter and corresponding current (J) is measured using ammeter. All the measurements have been recorded with current measurement range from 10^{-2} A to 10^{-12} A and maximum voltage upto 200 V at dark condition in ambient.

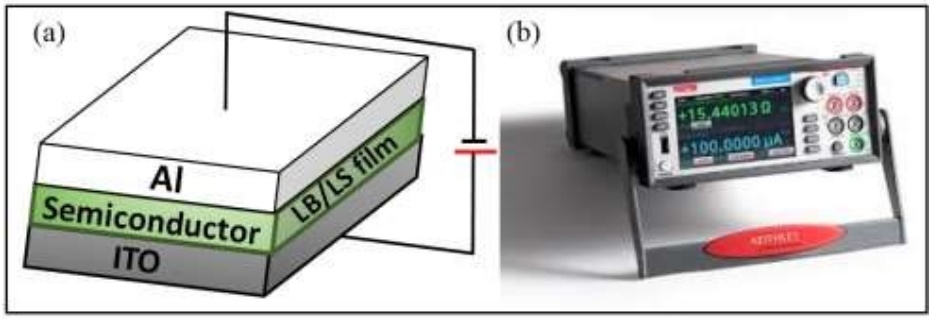

Figure 2.18 (a) Schematic diagram of ITO/Semiconductor LB (or LS) film/Al sandwiched structure, and (b) Photograph of sourcemeter.